Available online at www.sciencedirect.com
ScienceDirect
Comput. Methods Appl. Mech. Engrg. 196 (2007) 3279–3299
Computer methods in applied mechanics and engineering
www.elsevier.com/locate/cma

Shape optimization of 2D structures using simulated annealing

Fazil O. Sonmez *

Department of Mechanical Engineering, Bogazici University, Istanbul, Bebek 34342, Turkey

Received 13 September 2005; received in revised form 22 May 2006; accepted 11 January 2007
Available online 31 March 2007

Abstract

The goal of this study is to obtain globally optimum shapes for two-dimensional structures subject to quasi-static loads and restraints. For this purpose a technique is proposed, using which the volume (or weight) of a structure can be minimized. The emphasis is on how one can define the shape precisely, and find a shape that accurately reflects the globally optimum shape.

As design constraints, stresses developed in the structure should not exceed the maximum allowable stress, and connectivity of the structure should not be lost during shape changes. Optimization is achieved by a stochastic search algorithm called direct simulated annealing (DSA), which seeks the global minimum through randomly generated configurations. In order to obtain random configurations, a boundary variation technique is used. In this technique, a set of key points is chosen and connected by cubic splines to describe the boundary of the structure. Whenever the positions of the key points are changed in random directions, a new shape is obtained. Thus, coordinates of the key points serve as design variables. In order to apply the optimization procedure, a general computer code was developed using ANSYS Parametric Design Language. A number of cases were examined to test its effectiveness. The results show that this technique can be applied to two-dimensional shape optimization problems with high reliability even for cases where the entire free boundary is allowed to vary.
© 2007 Elsevier B.V. All rights reserved.

Keywords: Direct search simulated annealing (DSA); Boundary variation; Precision; Accuracy; FEM; 2D structures

1. Introduction

The increasing demand for lightweight, high-performance, low-cost structures, drives the considerable current research going on in the field of structural optimization. Studies on shape optimization [1–87] attest that shape changes may lead to considerable savings in weight and improvements in structural performance. Applications in this field include optimum shape designs of fillets [4,7,9,12,20,25,27,30,43,50,51,53,66,71,80,85,87], cams [61], holes in plates [3,7,9,10,12,19,22,25–28,32,39,41,42,60,66,73,76,80,83,85,87] for single and multiple [68] load cases, rings [30], torque arms [6,20,27,38,62,71,84], connecting rods [31,53,74,79,83], brackets [6,38,62,79,84], chain links [10,27,77], hooks [20,42], torque converter subject to pressure and centrifugal loads [69], uniaxially loaded plate with a hole [77], bridge under moving [76] and static [73] loads, plates containing cracks [37], plates with a notch [35,59,85], 2D structures subject to fatigue loading [74], 2D structures subject to thermomechanical boundary conditions [57], 2D structures containing a crack [55], various other 2D structures [39,48,65,70], saw blades [23], cantilever beams [21,24,28,29,35,41,53,60,64,70,88], beams subject to torsional loading [49], beams with thin-walled sections [44], axially excited beams [72], thin-walled tubes subject to torsional loading [77], shells under dynamic loading [67], components which are in contact [40,46,54,56,75,83], wheel profile of railway vehicles [81], thermal fins [17,58], axisymmetric structures [78], 3D structures like engine bearing cap [11], cantilevered thick plate with a hole though the thickness [16,47], aircraft turbine disk [16], control arm [63], engine mount bracket [63], and slider bearings [82].

The general purpose of shape optimization is to find the best profile for a structure under various constraints

* Tel.: +90 212 359 7196; fax: +90 212 287 2456.
E-mail address: sonmezfa@boun.edu.tr

0045-7825/$ - see front matter © 2007 Elsevier B.V. All rights reserved.
doi:10.1016/j.cma.2007.01.019

imposed by the requirements of the design. The optimum shape provides either the most efficient and effective use of material or the best performance. Accordingly, in some of the studies the goal was to minimize weight of the structure [10,11,16,17,20,24,25,30,31,35,38–41,48,49,51,53,62,69–71,77–79,84], in others to increase mechanical performance, e.g. to minimize stress concentration [3,19,22,25,26,32,33,42,43,57,60,66,68,77,83,87], maximize fracture strength [37,80,85], buckling strength [65], fatigue life [50,55,59,68], and heat flux [17,58], minimize peak contact stress [46,54,56,75,83], compliance [7,29,34,48,63,64,67,70,57,73,78], peak acceleration [67], and the probability of failure for brittle materials [23], and optimize dynamic behavior of structures [44,52,72,88].

In order to optimize a structure, some of its properties affecting the cost function should be changed. As for a shape optimization problem, the boundary should be allowed to vary. In previous studies, boundaries of the structures were usually defined by spline curves [9,11,23–25,28,31,35,39–41,46,47,51,56–61,65,66,69–71,76,77,87,88] passing through a number of key points. Positions of these points thus become design variables. NURBS curves [27] defined by a polygon can also be used to define a shape. Weights at each vertex of the polygon then become design variables. Some parameterized equations can be used for boundary curve [26,30,34]; the parameters then control the size, shape and aspect ratio of the boundary. The advantage of using these curves is that one may define the shape of the model using just a few design variables and obtain a smooth boundary. Alternatively, in a number of studies [3,32,43,64,68,83] all or some of the nodes at the boundaries were allowed to change their positions; or magnitudes of a set of fictitious loads on the boundary nodes were changed [10]; or more simply dimensions of individual parts of the structures were taken as design variables [29,52]. Also, by removing or restoring materials within the elements of the finite element model, the shape of the structure may be changed [20,26,49,74,75,80]. In that case, presence of material becomes a design variable.

During a shape optimization process, geometry of the structure may undergo substantial changes, such that it can no longer be considered as a viable structure, e.g. geometric model may become unfeasible [20,21], stresses may exceed the admissible stress level [20,21,24,29–31,35,38–41,51,62,71,78,79,84], fatigue life may be shorter than the lowest allowable number of cycles [74], natural frequency may be lower than a certain limit [24], displacements may be too large [11,16,24,35], finite element mesh may become too distorted [59], the area or volume may become too large [7,29,46,65,67,72,73,88], manufacturing may become too difficult [59]. In these cases, behavioral or side constraints should be imposed.

Locating globally optimum shape designs is a difficult problem, requiring sophisticated optimization procedures. In typical structural optimization problems, there may be many locally minimum configurations. For that reason, a downhill-proceeding algorithm, in which a monotonically decreasing value of objective function is iteratively created, may get stuck into a locally minimum point other than the globally minimum solution. Its success depends on the choice of initial design. The usual approach is to employ the algorithm many times starting from different configurations with the hope that one of the initial positions be sufficiently close to the globally minimum configuration, and then to choose the lowest value as the globally minimum solution. Another disadvantage is that if the starting point is outside the feasible region, the algorithm may converge to a local minimum within the infeasible domain.

If a downhill-proceeding local search algorithm is used, an optimization procedure can only be successful if it is used to improve the current design [4,69,83] or only a small segment of the boundary is allowed to move [3,4,9,12,19,26,28,35,39,43,53,69], or only a small number of dimensional parameters are used to define its shape [6,26,29,30]. The advantage of using these algorithms, on the other hand, is their computational efficiency. Just a small number of iterations are needed to obtain an improved design.

One of the optimization methods that have been used to obtain optimum structural designs is evolutionary structural optimization. The approach is to gradually remove inefficient materials until the shape of the structure evolves into an optimum. Although this method is not a global search algorithm, because of its simplicity and effectiveness, it has been applied to many structural optimization problems [49,74–76,80]. This method is also suitable for topology optimization, where not only outer boundary but also geometry of inner regions is allowed to change. There are also similar algorithms which can effectively be used to find improved designs such as biological growth methods [19,38,66] and metamorphic development methods [78].

In order to find the absolute minimum of an objective function without being sensitive to the starting position, a global optimization method has to be employed in structural optimization problems. Stochastic optimization techniques are quite suitable in this respect. Among their advantages, they are not sensitive to starting point, they can search a large solution space, and they can escape local optimum points because they allow occasional uphill moves. The genetic algorithm (GA) and simulated annealing (SA) algorithm are two of the most popular stochastic optimization techniques.

Genetic algorithms found many applications on shape optimization problems [15,21,31,41,47,48,61,64,70,57,77,79]. They are based on the concepts of genetics and Darwinian survival of the fittest [13]. The idea is to start the search process with a set of designs, called population. The search procedure is a simulation of the evolution process. The genetic algorithm transforms one population into a succeeding population using operators of reproduction, recombination, and mutation. The convergence to the global minimum depends on the proper choice of the design parameters, rules of the reproduction and mutation.

Kirkpatrick et al. [89] first proposed simulated annealing (SA) as a powerful stochastic search technique. The main

advantage of SA is that it is generally more reliable in finding the global optimum, i.e. the probability of locating the global optimum is high even with large numbers of design variables. Application of simulated annealing to shape optimization of the structures is quite rare. Anagnostou and his coworkers [17] used SA to design a thermal fin with minimum material use. Shim and Manoochehri [20] used SA to obtain optimal designs for two-dimensional structures with a minimum use of material. In their approach, a structure was first divided into a number of small finite element blocks and then these blocks were randomly removed or restored to obtain a randomly generated new shape. One difficulty with this method is that removing and restoring an element may violate model connectivity. Whenever a new configuration is generated its connectivity should be checked by a complicated algorithm. Another difficulty is the roughness of the resulting boundaries. If smooth boundaries are desired, small elements should be used, resulting in long computational times. However, their study demonstrated the promise of SA in solving shape optimization problems.

The ultimate goal of a designer in using a shape optimization algorithm is just to state the boundary conditions and let the algorithm do some iterations without human intervention and automatically produce the best design. In this respect, the previous studies had only a relative success. Many of them relied too much on designer's intuition, or imposed tight restrictions on the movements of boundary, or fixed some portions of boundary so that the number of possible designs among which the algorithm may search the optimum one was quite limited. This study attempts to come one step closer to our ultimate goal. The procedure developed in this study may start from almost any initial model thanks to the global search algorithm used. In fact the only interactive effort required from the designer is to provide an initial coarse boundary model consisting of spline curves passing through the given key points, and to specify the boundary conditions and which key points of the boundary are allowed to move during the optimization process.

Another requirement for the search of globally optimum configuration is the precise definition of the optimized system. If the system is complex, complete definition of it may require large numbers of design variables. If all of them are used as optimization variables, that means if the optimized system is precisely defined, long computational times are needed, and also likelihood of locating the optimum design may become very low. If the definition of the system is based on a limited number of design variables, that means if the definition allows for only a limited number of distinct configurations, the resulting optimum configuration may not reflect the best possible design. Although using the most precise definition of the system during optimization is desirable, this is usually not practicable; but if a less precise definition is used, one should be aware of its impact on how well the final design represents the best possible design. To the author's knowledge, there is no study on structural optimization, or specifically on shape optimization in which precision was a main concern. Apparently, in most of the previous studies, definition of shape was not precise enough to be capable of representing the best possible shape. In this study, on the other hand, a procedure is proposed to monitor precision so that a reasonable compromise can be made between a better definition and a shorter computational time.

Another concern in shape optimization is the accuracy, i.e. how well the resulting optimum shape reflects the best possible shape. In many of the previous studies, the goal was to improve an intuitively found current design through a local search algorithm rather than to find the best possible shape. In some of them, global search algorithms were used, but the accuracy remained questionable. In this study, a number of methods are proposed to achieve high accuracy.

2. Problem statement

Consider a two-dimensional structure as in Fig. 1 having a geometry that can be defined by its boundary and thickness. The structure is subject to in-plane quasi-static loads; it is also restrained from moving at some points of the boundary. Applied loads and restraints are considered as boundary conditions. The structure should be able to resist the loads without failure. This means the material should not yield. Besides, no part of the structure is to lose its connection to the restraints; i.e. the structure should remain in one piece. These are the two constraints imposed on the structure. Our objective is to minimize the volume (or weight) of the structure, in other words, to obtain a configuration (shape) with the most efficient use of material without violating the behavioral and geometric constraints.

The shape optimization problem for minimum weight can be formulated briefly as

Given:	initial positions of key points, boundary conditions (applied forces and restraints), material properties
Find:	the optimum shape of the structure
Minimize:	$V =$ volume of the structure
Subject to:	(i) the stress constraint ($\sigma_{\max} \leqslant \sigma_{\text{allow}}$) (ii) the geometric constraint (model connectivity)
Design variables:	the positions of the key points

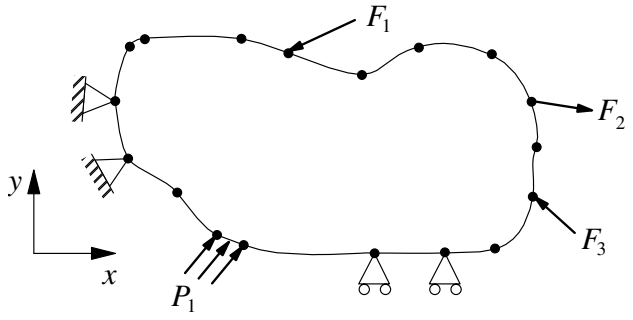


Fig. 1. Representation of a 2D shape optimization problem.

This means that the maximum equivalent (Von Mises) stress of the structure, σ_{max}, should be less than or equal to the maximum allowable stress, σ_{allow}, and the key points which are used to define the boundaries of the structure should move without any loss in model connectivity.

3. Problem solution

In this study, direct search simulated annealing (DSA), proposed by Ali et al. [90], is adopted. This is an improved version of simulated annealing. SA gets its name from the physical process whereby the temperature of a solid is raised to a melting point, where the atoms can move freely and then slowly cooled. The method attempts to model the behavior of atoms in forming arrangements in solid material during annealing. Although the atoms move randomly, as their natural behavior they tend to form lower-energy configurations. However, this is a time-driven process. When a material is crystallized from its liquid phase, it must be cooled slowly if it is to assume its highly ordered, lowest-energy, perfect crystalline state. At each temperature level during cooling, the material should reach equilibrium. As the temperature decreases, the arrangement of the atoms gets closer and closer to the lowest-energy state. This process continues until the temperature finally reaches freezing point.

There is an analogy between a physical annealing process and an optimization process. Different configurations of the problem correspond to different arrangements of the atoms. The cost of a configuration corresponds to the energy of the system. Optimal solution corresponds to the lowest-energy state. Just in the same manner the atoms find their way to build a perfect crystal structure through random movements, the global optimum is reached through a search within randomly generated configurations.

In SA, an arbitrary initial design is selected and systematically updated until a stopping criterion is satisfied. Updating is based on an iterative procedure. In each iteration, an arbitrary design is generated in the neighborhood of the current configuration. If the cost function of the new design has a smaller value compared to that of the current design, it is accepted. The new design then replaces the old one. On the other hand, if the new cost function has a larger value, the acceptability of the design is decided according to the probability of Boltzmann distribution. The calculation of this probability depends on a temperature parameter, T, which is referred to as temperature, because it plays a similar role in the optimization process as the temperature in the physical annealing process. The temperature is kept constant for a number of trials and then reduced. The rate of reduction should be slow so as not to get trapped at a locally minimum point. At initial stages of the algorithm (at high temperatures), the probability of accepting worse designs is higher but later on at low temperatures, this probability becomes lower and lower so that in the end the designs having a higher cost are almost never accepted.

DSA differs from SA basically in two aspects. Firstly, DSA keeps a set of current configurations rather than just one current configuration. Secondly, it always retains the best configuration. In a way, this property imparts a sort of memory to the optimization process. If a newly generated configuration is accepted, it just replaces the worst configuration.

3.1. The cost function

Because the thickness of the structure is fixed and only its lateral area is allowed to vary, the objective function to be minimized may be taken as its area instead of its volume. Shape optimization is a constrained optimization; but SA is only applicable to unconstrained optimization problems. By integrating a penalty function for constraint violations into the cost function, the constrained optimization problem can be transformed into an unconstrained problem, for which the algorithm is suitable. A combined cost function may be constructed as

$$f = \frac{A}{A_{ini}} + c\left\langle \frac{\sigma_{max}}{\sigma_{allow}} - 1 \right\rangle^2. \tag{1}$$

Here, the bracketed term is defined as

$$\left\langle \frac{\sigma_{max}}{\sigma_{allow}} - 1 \right\rangle = \begin{cases} 0 & \text{for } \sigma_{max} \leqslant \sigma_{allow}, \\ (\sigma_{max}/\sigma_{allow}) - 1 & \text{for } \sigma_{max} > \sigma_{allow}, \end{cases} \tag{2}$$

where A_{ini} is the area of the initial configuration; c is a weighing coefficient, for which a value about 0.9 was found to be satisfactory. Any excursion into the infeasible region ($\sigma_{max} > \sigma_{allow}$) results in an increase in the cost function. On the other hand, if model connectivity is lost, the new configuration is never accepted, and therefore there is no need to calculate its cost function.

3.2. The boundary variation technique

SA requires random generation of a new configuration (in our case, a new shape) in each iteration. Definition of a configuration should be made based on optimization variables. The algorithm tries to find the optimum values of these variables, which define the best configuration. Shape of a 2D-structure is defined by its thickness and boundary. Accordingly, its shape can easily be described by spline curves passing through a number of key points. Some of these points may be fixed, while others are allowed to move during optimization. As illustrated in Fig. 2, whenever the positions of the moving key points are changed in random directions through random distances, a new boundary, thus a new configuration is obtained. Accordingly, the x and y coordinates of the moving key points become optimization variables. Model connectivity is ensured by just checking whether or not the spline segments of the boundary cross over or touch each other, which is automatically done by the FE software.

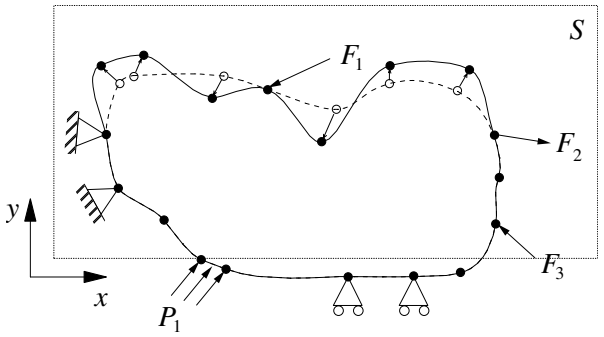


Fig. 2. Generation of a random configuration through random movements of key points.

Key points are allowed to move only within a region, S, defined by the designer. Although search of the global minimum without restricting the movements of the key points is possible, computational time becomes unnecessarily much longer. Search domain should not be too restrictive, but should exclude the regions that are definitely expected to be far away from the boundary.

For the direction of movement, a random real number between 0 and 360, for the moving distance a random number between 0 and $R_{\max}$ is chosen. Here $R_{\max}$ is the maximum moving distance. Our experience has shown that in order to search the global optimum within a large region, instead of giving small perturbations to the current configuration to obtain a new configuration in the near neighborhood of the current one, we should allow a large variance in the current configurations. For this reason, the magnitude of $R_{\max}$ is taken as 10% of the square root of the searched area, S; thus each key point can move up to a distance of about 10% of average dimension. This means that the neighborhood of a current configuration where a new configuration is generated is initially quite large. This can also be considered as a logical consequence of simulating the physical annealing process, where mobility of atoms is large at high temperatures. Also, as in the physical process, where mobility of atoms decreases as the temperature is lowered, moving distance is reduced as the temperature parameter is decreased; but the reduction scheme does not directly depend on temperature. The configuration that is worse than all current configurations except the worst one is defined as the worse configuration, and if no improvement is made on the worse shape during a Markow chain, $R_{\max}$ is reduced by 0.5%.

3.3. The set of current configurations

DSA unlike ordinary SA starts with a set of N configurations, A, rather than starting with only one configuration. For the shape optimization problem, the initial set of N different shapes is selected randomly within the search domain, S, without any regard to cost, but connectivity is observed. Their costs are calculated and stored. The highest and lowest cost function values are denoted as f_h and f_ℓ. The number of these configurations depends on the dimension of the problem:

$$N = 7(n+1), \tag{3}$$

where n is the dimension of the problem, i.e. the number of design variables. Since x and y coordinates of the moving key points are the variables defining the shapes, in our case n is given by

$$n = 2n_m, \tag{4}$$

where n_m is the number of moving key points. This means that for each additional moving key point, one must generate 14 more current configurations.

3.4. Generation mechanism

In each iteration, first, a configuration is randomly selected from the set of current configurations, and then random displacements are given to the moving key points, resulting in a new shape. If any of the moving key points falls outside the search domain S (Fig. 2), this process is repeated until all of the moving key points fall within S. During movements of the key points if one segment of the boundary crosses another one, or they touch each other, connectivity is lost. In that case, the generation process is repeated.

3.5. Acceptability

Acceptability of a new configuration depends on the value of its cost function, f_t; its acceptability, A_t, is calculated by

$$A_t = \begin{cases} 1 & \text{if } f_t \leqslant f_h, \\ \exp((f_h - f_t)/T_k) & \text{if } f_t > f_h \end{cases} \tag{5}$$

here f_h is the highest cost function value in A. This means every new design having a cost lower than the cost of the worst design is accepted. But, if the cost is higher, the trial configuration may be accepted depending on the value of A_t. If it is greater than a number randomly generated between 0 and 1, the trial configuration is accepted, otherwise rejected.

If the trial function is accepted, it replaces the worst configuration. The best configuration, thus, always remains in A. In each iteration, f_h and f_ℓ are updated. At high temperatures it is unlikely that A will form a dense cluster. At low temperatures, because the likelihood of accepting a worse configuration is low, A will shrink to form a dense cluster.

3.6. Cooling schedule

The simulated annealing process consists of first "melting" the system being optimized at a high "temperature", T, then lowering the temperature slowly until the system "freezes" and no further changes occur. Here, temperature, T, has no physical meaning; it is just a control parameter. Melting corresponds to the initial stage at which

configurations are generated within the solution domain, S, without much regard to the cost. At high temperatures, (high values of T) the probability of acceptance is high as Eq. (5) implies. Accordingly, configurations that have even very high cost values may be accepted, just as in the physical annealing process the atoms in the melting state may form configurations having very high energy. At low values of temperature parameter, acceptability becomes low and acceptance of worse configurations is then unlikely, just as the atoms become stable, and do not tend to change their arrangements at low temperatures. The cooling schedule in SA controls the convergence of the algorithm to the global minimum just as the cooling scheme in the physical annealing process controls the final microstructure. Therefore, performance of SA depends on the cooling schedule.

In a cooling schedule, first an initial value, T_0, should be specified for the temperature parameter. A scheme is then required for reducing T and for deciding how many trials are to be attempted at each value of T. Lastly, the freezing (or final value of the) temperature parameter is specified.

Initial value of the temperature parameter: Its initial value should be high enough to allow nearly all trials to be accepted. This provides complete "melting" at the initial stages of the optimization process. Otherwise, the region will not be thoroughly searched and thus the algorithm may become trapped in a local minimum. In the physical analogy mentioned earlier, choosing high T_0 corresponds to heating up the solid until all particles are randomly arranged in the liquid phase such that atoms may freely arrange themselves.

Length of the Markow chains: Iterations during which the value of the temperature parameter, T, is kept constant are called Markov chains (or inner loops). Ali et al. [90] adopted the following equation to decide on the length of a Markow chain (the number of trials (or iterations)) for the kth level of T:

$$L_k = L + L(1 - \mathrm{e}^{f_\ell - f_\mathrm{h}}). \tag{6}$$

Here

$$L = 10n, \tag{7}$$

where n is the dimension of the problem given by Eq. (4). At high temperatures, the current configurations form a sparse cluster; consequently $f_\mathrm{h} - f_\ell$ is large and Markow chain length is close to $2L$. On the other hand, when they form a dense cluster at low temperatures, it approaches to L. During the execution of kth Markow chain with length L_k, if a configuration is generated having a cost less than f_ℓ, the best value in A, the current chain is stopped, and a new Markow chain is started. If a configuration better than the best configuration in A is not found, the complete chain of length L_k is executed.

The scheme for decreasing the temperature parameter: After the initial value of the temperature parameter, T_0, is determined, a decrement rule must be established to find the subsequent values of the temperature parameter. The probability of reaching the global optimum solution depends on how fast the value of the temperature parameter is lowered. If the cooling rate is fast, the optimization process will probably end up with one of the higher-cost local minima. If the cooling rate is slow, the reliability of finding the global optimum solution will be high, but, the optimization process will take excessively long time. Therefore, the choice of the cooling schedule determines the effectiveness of the algorithm.

In DSA, a temperature scale factor, (α_{k+1}), is specified to calculate the value of the temperature parameter in the next Markow chain, T_{k+1}.

$$T_{k+1} = \alpha_{k+1} T_k, \tag{8}$$

where T_k is the value of the current temperature. A value for $\alpha_{k+1} \in [\alpha_{\min}, \alpha_{\max}]$ is calculated using the following equation [90]:

$$\alpha_{k+1} = \begin{cases} \alpha_{\max} & \text{if } L_k > L'_k, \\ \alpha_k - (\alpha_k - \alpha_{\min})(1 - L'_{k-1}/L_k) & \text{else if } L_k > L'_{k-1}, \\ \alpha_{\max} - (\alpha_{\max} - \alpha_k)(L_k/L'_{k-1}) & \text{else } L_k \leqslant L'_{k-1}, \end{cases} \tag{9}$$

where L'_k is the actual number of trials executed in the kth Markow chain. If no configuration is found in the kth Markow chain (inner loop) that is better than the best current configuration L'_k is set to the value of L_k. If a configuration which is better than all is found, the inner loop is terminated, and L'_k is set to the number of iterations actually executed in this loop. In this study, $\alpha_{\max} = 0.999$ and $\alpha_{\min} = 0.99$ were chosen as appropriate values, which provided a compromise between the two effectiveness criteria, i.e. short computational time and high reliability of locating global minimum. Initial value of α is taken as the average of $\alpha_{\max}$ and $\alpha_{\min}$.

Because, a new configuration is generated by giving perturbations to a configuration selected randomly among a large number of current configurations, and once accepted the new configuration replaces only the worst one, cooling rate has less importance in DSA in comparison to conventional SA. The worst configuration seldom plays a role in the generation process. Again, it is important to start with a temperature high enough to accept almost all generated configurations.

Stopping criterion: The optimization process is terminated when no further appreciable improvement can be achieved. This occurs when three conditions are satisfied. Firstly, the current temperature parameter should be small, in other words it should be close to the "freezing temperature" (zero), i.e. no further worse designs may be accepted. Secondly, the current configurations, A, should form a dense cluster; thus all alternatives were eliminated and optimization process converged to a single configuration. Thirdly, the maximum moving distance of key points, $R_{\max}$, should be small; this means the neighborhood of the current configurations within which optimum design is sought became very small. Accordingly, the stopping criterion can be expressed as

$$f_{\mathrm{h}} - f_{\ell} < \varepsilon_1 \quad \text{and} \quad T_k < \varepsilon_2 \quad \text{and} \quad R_{\max} < \varepsilon_3, \tag{10}$$

where ε_i are small numbers. For the optimization problems that were considered, it was more than sufficient to take $\varepsilon_1 = \varepsilon_2 = 0.0001$, and $\varepsilon_3 = 0.05$ mm for a good estimate of the global minimum. The value of ε_3 depends on the dimensions of the structure.

3.7. Solution procedure

As a first step in the optimization procedure, the designer defines the force and displacement boundary

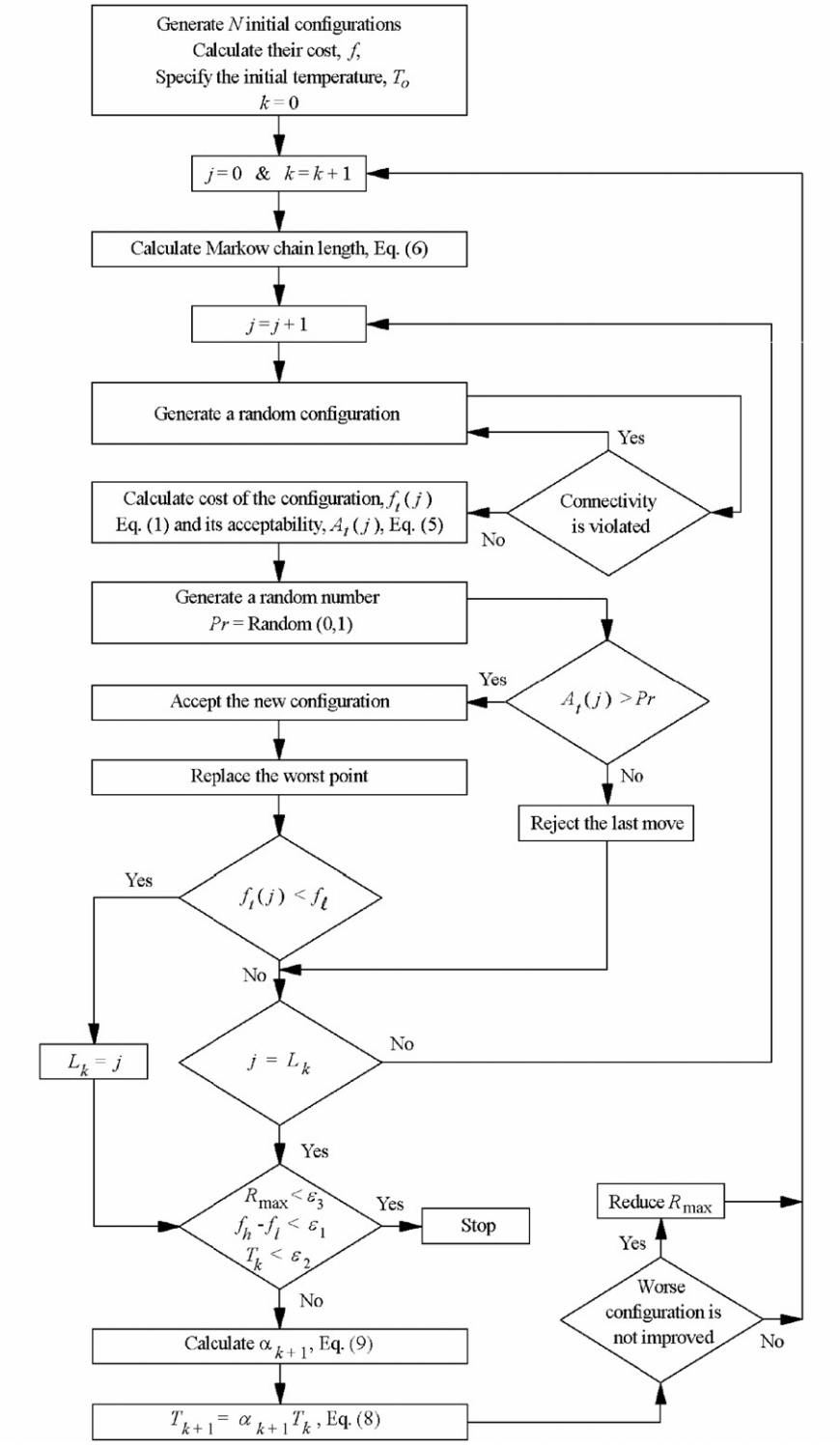


Fig. 3. The solution procedure.

conditions, chooses the material, and decides on the number of key points, the moving boundaries and how they are connected. Fig. 3 describes the procedure followed in this study to solve the optimization problem. First, N number of initial configurations are randomly generated within the search domain, S; their costs are calculated and the best, worse, and worst ones are determined. An initial value for the temperature parameter is chosen, which should be high enough to accept nearly all randomly generated new shapes. In the figure, k and j show the inner loop (Markow chain) number and the number of generated configurations in the current inner loop, respectively. In each iteration of the Markow chain, a new configuration is generated within the search domain, S, by giving random displacements to the key points of a randomly chosen current configuration. If a key point falls outside S, random repositioning of this key point is repeated. If connectivity is lost, the generation process is repeated until a valid geometry is obtained. If the acceptability of the new configuration calculated by Eq. (5) is greater than a randomly generated number, it is accepted, replacing the worst configuration. If its cost is lower than the best cost, the inner loop is terminated; otherwise the iterations are continued until the iteration number, j, becomes equal to L_k calculated by Eq. (6). When an inner loop ends, the temperature parameter is decreased. With a lower temperature, acceptability decreases as Eq. (5) implies. This means that a configuration having a cost higher than the cost of the worst configuration is less frequently accepted.

As in the physical annealing process where the mobility of the atoms diminishes during cool down, mobility of the key points is decreased as acceptability decreases. This is done when a configuration is not found during a Markow loop which is better than the worse current configuration. In this way, the neighborhood of the current configurations within which a new configuration is generated narrows down as acceptability becomes lower and lower. If a shape having a cost lower than the cost of the worse current configuration is not found during the inner loop iterations, the maximum moving distance, $R_{\max}$, is reduced. The optimization process is continued until three stopping criteria stated in Eq. (10) are satisfied.

4. Accuracy of an optimum design

The measure of accuracy for an optimum configuration is the degree of how well it represents the best possible design.

As one of the sources detracting from the accuracy, search algorithm may get stuck into one of the local optimums that fail to approximate the global optimum. One may not ensure that the resulting configuration is globally optimal, but may use relatively reliable search algorithms such as simulated annealing. With a good choice of optimization parameters, one may achieve reliability greater than 90% at the same time avoid excessively long computational times.

Another source of low accuracy is due to errors in calculating the cost of a configuration [35,86]. In many structural optimization problems, maximum stress value is used either in calculating the cost function or in checking constraint violations. Designers usually carry out a finite element (FE) analysis to calculate the stress state in the structure, but they tend to choose a rough FE mesh to alleviate the computational burden. However, this may lead to erroneous values of stress, and the resulting design, as shown before [86], will not even be similar to the globally optimum design.

Imprecise definition of shape also leads to optimal shapes not similar to the best possible shape, which will be discussed next.

5. Precision of an optimum design

How well the optimized system is defined by the design variables is a measure of precision. Some of the parameters that define the system are allowed to be changed during an optimization process. The number of these parameters and the range of values they may take determine the degree at which the system can be tailored to the best performance. By increasing the number of design variables and range of their values, one may obtain a better definition and also a better optimum design. In the shape optimization problem, by using a larger number of moving key points, one may better describe the boundary, i.e. shape of the structure, and minimize its volume to a larger extent. However, the chances of locating the globally optimum design become lower and lower as the number of design variables increases, at the same time computational times get longer and longer. With a large number of optimization variables, locating the global minimum becomes difficult. As the designer tries to obtain a more precise definition, he or she becomes less sure of the accuracy of the results. One may repeat the optimization process many times and designate the design having the lowest cost as the global optimum design. However, because of long computational times this approach is not feasible. Another way to overcome this difficulty is to start optimization by choosing only a few design variables and finding the optimum design. In this case, the reliability of locating globally optimum design will be high, even though precision will be low. Then, the designer keeps increasing the number of variables and finding the optimum designs. With the assumption that the discrepancy between the successively obtained optimum designs will not be large as the number of design variables is increased, one may observe convergence to the most precise globally optimum design.

6. Results and discussions

The optimization algorithm was implemented using the parametric design language of ANSYS. By just executing its commands, key points and spline curves are generated, connectivity of the model is checked, the area bounded by

these curves is calculated, a completely new finite element mesh is automatically generated in each iteration, and the maximum equivalent stress and cost are calculated.

In all the problems that were considered, the material of the structure was steel with an elastic modulus of 207 MPa and Poisson's ratio of 0.28 and the structure was in plane-stress condition. Stresses were assumed to be within the linearly elastic region of the stress–strain curve.

6.1. Optimal design of an eccentrically loaded plate

One of the problems that were considered in this study is the optimal design of an eccentrically loaded plate restrained at one end and loaded at the other (Fig. 4). One segment of the border on the right is fixed in length and subject to 200 MPa pressure. The left border is defined by a line between two key points; the lower one is fixed, while the upper one is free but restrained to move in the vertical direction. The search domain, S, within which the key points can move, is defined by a rectangle of dimension 10 cm × 12 cm. The allowable stress of the material is taken as 300 MPa.

First, five key points were used to describe the boundary and using their coordinates as design variables the best shape was found. Fig. 5 shows the optimal shape with its finite element mesh. The cross-section becomes larger and larger away from the loaded regions due to increased bending moment. Because the number of design variables was low, the optimum design could be obtained with high reliability. Then, optimization process was repeated using seven and nine moving key points resulting in the optimum designs shown in Figs. 6 and 7. The maximum moving distance, R_{max}, was initially 1.00 cm, and at the end of the optimization process, it decreased to a value of 0.036 mm. In this way, the algorithm could search a large region initially, and a close neighborhood towards the end of the optimization. The lateral areas of the optimum shapes defined by five, seven, and nine key points turned out to be 37.100, 36.313, and 35.903 cm^2, respectively. Consequently, with a higher number of key points, we could obtain a more precise definition of shape and also find an optimum configuration with a lower cost. Even though reliability of the solution becomes low with a large number of design variables, because it approximates the more reliable optimum designs defined by smaller number of key points, the reliability is ensured.

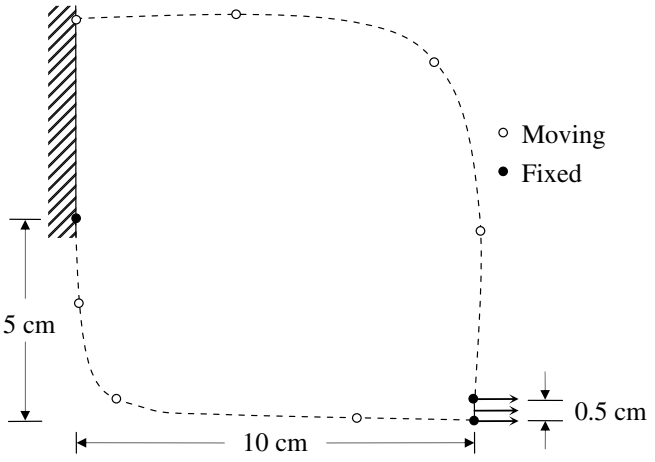


Fig. 4. Optimum design problem for an eccentrically loaded plate.

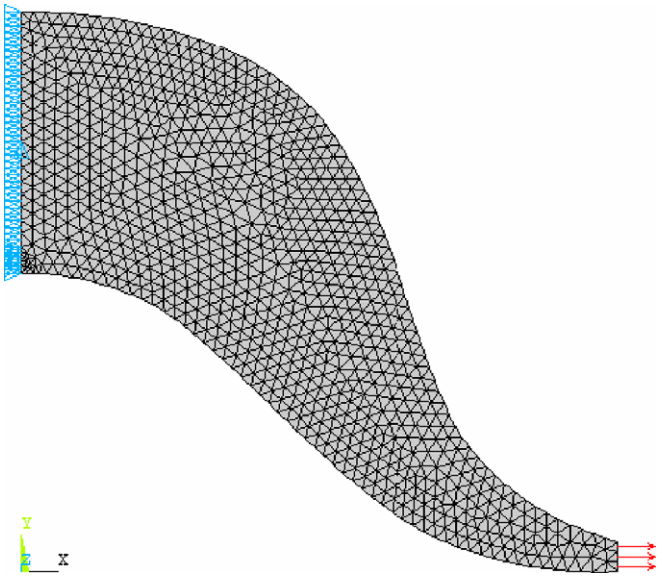


Fig. 5. The optimal shape of the eccentric plate defined by five key points.

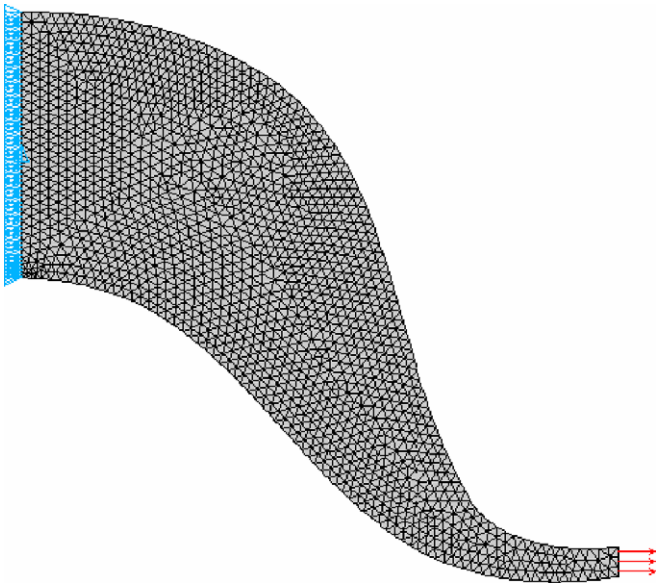


Fig. 6. The optimal shape of the eccentric plate defined by seven key points.

In order to ensure the accuracy at which the cost was calculated, convergence of the FE solution was frequently checked during the optimization process. If the change in the magnitude of the maximum stress was greater than 0.5% when FE analysis of currently best configuration was carried out using one fourth of the current size of finite elements, then the FE mesh was refined. The significance of

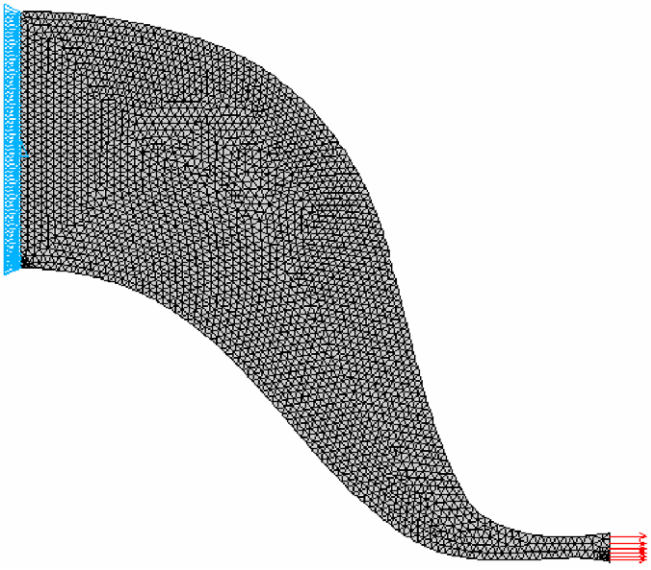


Fig. 7. The optimal shape of the eccentric plate defined by nine key points.

accuracy in FE calculations is better seen in Fig. 8, which shows the optimum shape obtained when a rough mesh is used. Although the error in stress level is only 5%, the discrepancy in shape was quite large.

6.2. Optimal design of a hook

Another problem considered in this study is the optimal design of a plate restrained at the top edge, and loaded over an arc of surface as shown in Fig. 9, which corresponds to loading of a hook. The half circle has a radius of 1.5 cm. This curved border is fixed in length and subject to 150 MPa pressure at the center decreasing to zero magnitude toward the sides. The restrained top border is defined by a line between two key points; both of them are free to move, but only in the horizontal direction and symmetrically such that their midpoint retains its position. The rest of the key points on the border are free to move within a search domain, S, of dimension 13 cm × 18 cm. The allowable stress of the material is taken as 800 MPa.

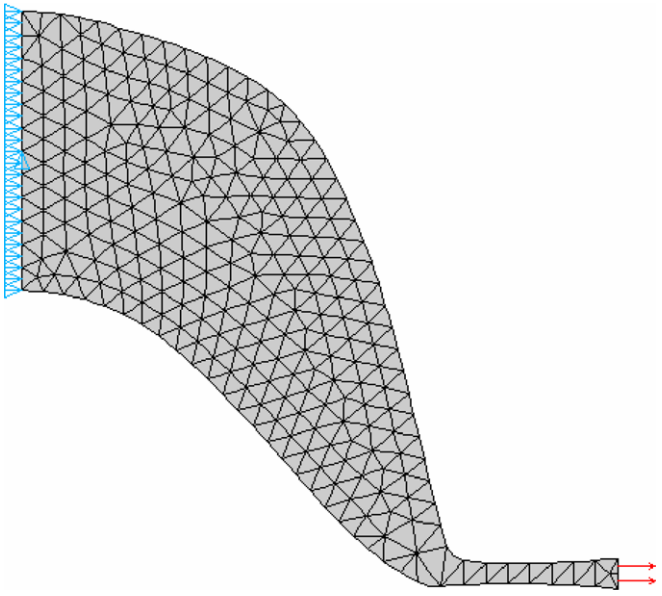


Fig. 8. Inaccurate optimal shape obtained with a rough mesh.

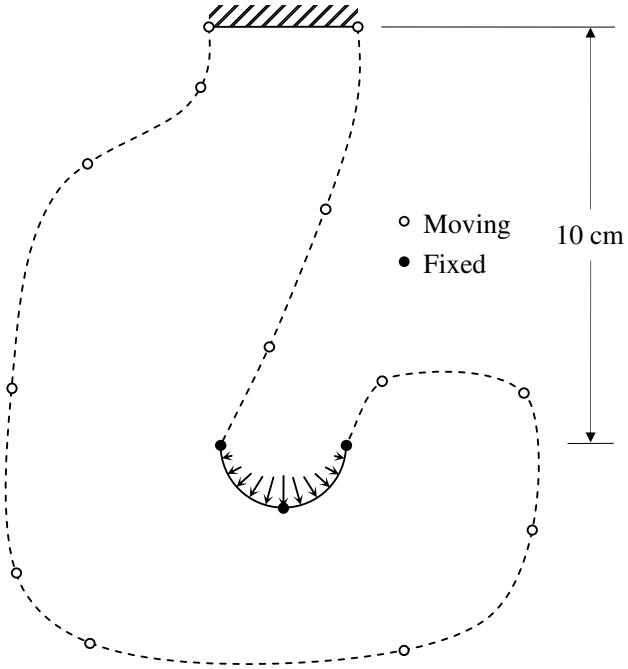


Fig. 9. Optimum design problem for a hook.

At the start of the optimization, initial current configurations are created by describing spline curves through key points randomly generated within the search domain, S. They are then ordered with respect to their cost; the ones having the lowest and highest costs are named as the best and worst configurations, respectively. Fig. 10 shows some these initial configurations created for the optimum hook design problem including the best (Fig. 10a) and worst (Fig. 10b) ones.

Fig. 11 shows the optimal shapes obtained using 6, 8, 10, 12, and 13 moving key points. The lateral areas of them are 37.888, 34.343, 33.959, 33.077, and 33.412 cm^2, respectively. When the number of key points is too large, locating the global minimum becomes extremely difficult. More or less the same curve can be generated by many different sets of key points. Then, there could be numerous near global optimum designs. For this reason, the algorithm may get stuck into one of them as in this case. The optimum shape defined by 13 key points is worse than the one defined by 12 key points. In these cases, one may start at a higher temperature and decrease the reduction ratio of the maximum moving distance to increase the probability of convergence to a better design at the expense of longer computational times; but there is a more effective method to be discussed later.

The maximum moving distance, R_{max}, was initially 1.60 cm, and towards the end of the optimization process, it decreased to a value of 0.092 mm. The upper regions of the hook are subject to pure axial load; for this reason they

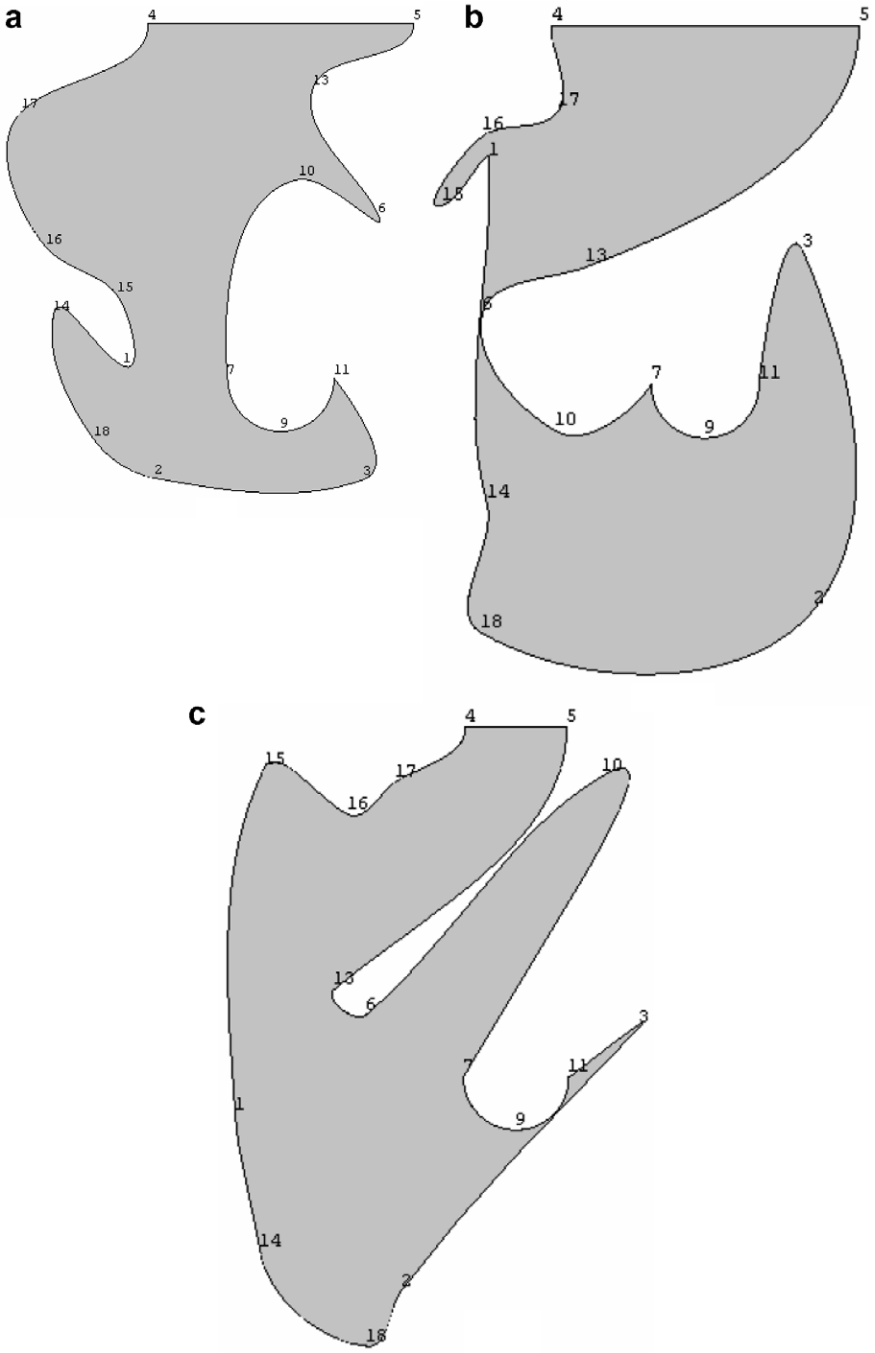


Fig. 10. Some of the initial current configurations generated randomly for the optimum hook design problem. The first one (a) and the second one (b) represent the best and worst configurations among them, respectively.

have the smallest cross-section. The other sections are subject to axial as well as bending moments. Because structures are far weaker against bending, and also because of stress concentration due to curved and varying cross-sectional areas, these regions have large cross-sections. One should also note that, although the resulting shape design is optimum for the given loads, it can barely be considered as a good design. The sharp corner can easily be broken during service. This optimization problem as stated above is considered only to see the effectiveness of the algorithm. In a more realistic optimum shape design, the loads that can be accidentally applied on the corner should be considered. Besides, one should consider a more realistic distribution of the contact forces.

It should also be noted that the failure criterion ($\sigma_{\max} > \sigma_{\text{allow}}$), which was also adopted in the previous studies for statically loaded structures made of ductile materials, even though easy to apply, is not appropriate in real life design problems. The failure mode of components made of ductile materials is large permanent deformation. This occurs when the nominal stress at a section exceeds the yield strength of the material. For this reason,

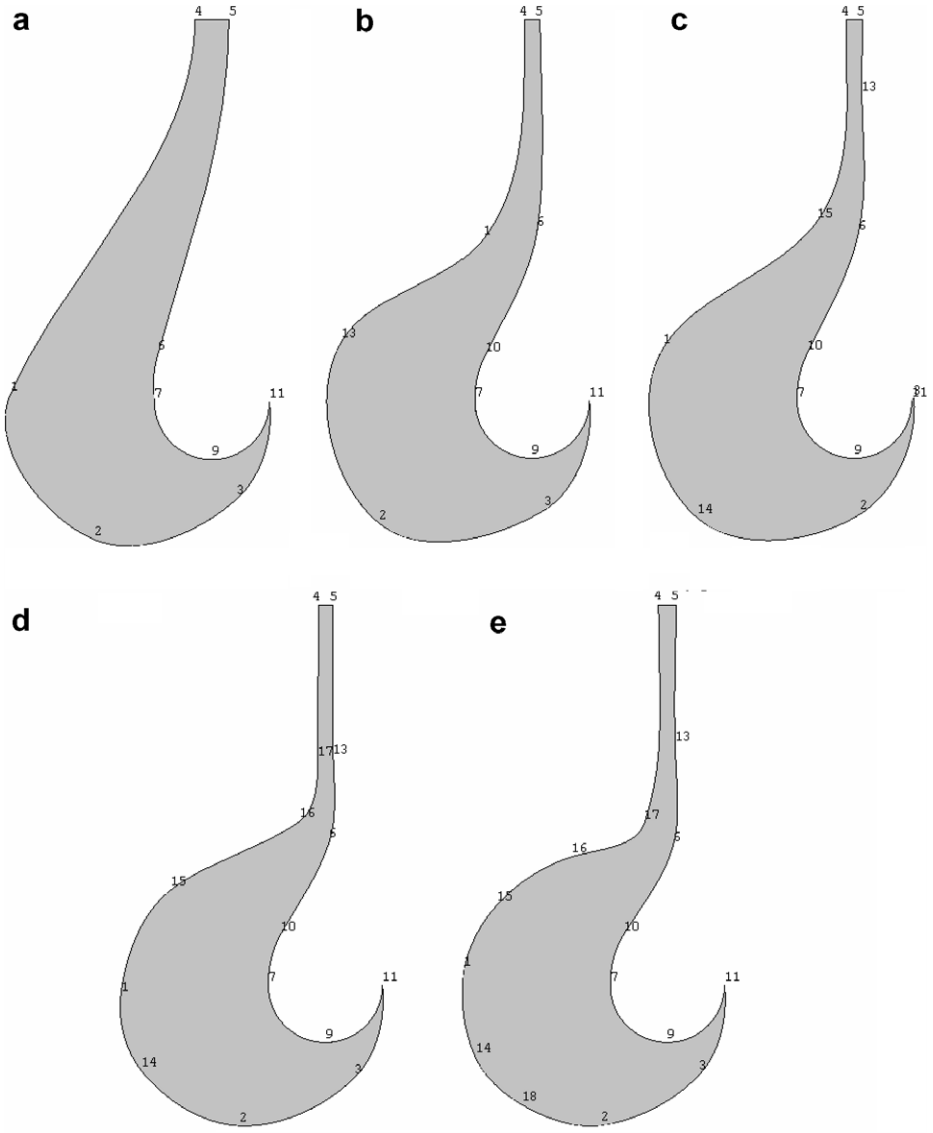


Fig. 11. The optimal shapes found using 6 (a), 8 (b), 10 (c), 12 (d), 13 (e) key points.

stress concentration effects are neglected. In our case, the maximum stress not nominal stress is used in the failure criterion. The optimum design reflected this choice. If an overload occurs, curved regions locally yield, but the section mainly remains elastic, and holds on. On the other hand, in the straight portion, where stress state is uniform, entire cross-section yields. Catastrophic failure, which occurs when the maximum stress exceeds ultimate stress, should also be expected to occur first in the straight portion. For this reason, the straight portion is weaker, and its cross-section should be made larger. The shape can be considered to be optimum, only if the material is brittle or the component is subject to fatigue loading.

6.3. Optimal design of a pin-joint

Another problem considered in this study is the optimal design of a pin-joint. Fig. 12 shows a typical pin-joint. The problem is to find the minimum-weight pin-joint that will not fail under static loading. The magnitude of the load is taken to be 200 MPa at the center of the contact zone decreasing to zero towards the end. Radius of the circular holes is 1 cm, and the distance between their centers is 13 cm. During the optimization process, the entire outer boundary is allowed to vary. Because of symmetry, only one quarter of the component is considered for analysis as shown in Fig. 13. The slope of the spline curve is set to 90° at the top, 0° at the bottom in order to ensure symmetry. The key points at these locations are free to move; but one only in the horizontal direction, the other only in the vertical direction. The search domain, S is defined by a rectangle of dimension 4 cm × 11 cm. The allowable stress of the material is taken as 300 MPa.

Fig. 14 shows the optimal shapes obtained using 4, 6, 8, and 10 moving key points. The lateral areas of them were 13.757, 12.603, 11.948, and 11.895 cm^2, respectively. The



Fig. 12. A typical pin-joint.

maximum moving distance, R_{max}, was initially 8 mm, and towards the end of the optimization process, it decreased to a value of 0.031 mm. The resulting optimum shape is somewhat surprising. This does not look like any of the commonly used pin-joints. A curved indent appears at the side of the hole. Although this may look strange, it is not counter to engineering intuition. We may assume that the curved indent tends to reduce the stress concentration effect of the curvature of the hole.

Fig. 15 shows the variation of the lateral area of the best configuration defined by eight key points during the optimization process. Convergence to optimum design may require hundred thousands of iterations. Even though simulated annealing does not require sensitivity analysis, computational burden is considerable. Nevertheless, ever increasing computational capacities made this algorithm a viable approach. It takes a week for a Pentium IV computer to generate the optimum shape defined by eight moving key points. Even so, ways of increasing computational efficiency will be discussed in the following section.

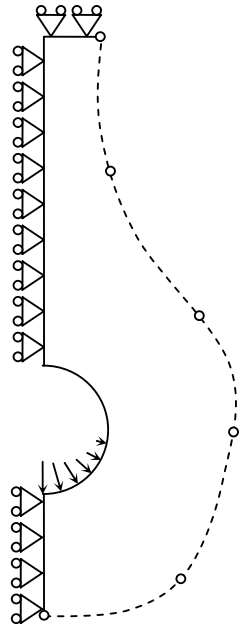


Fig. 13. Domain of analysis for the pin-joint and the boundary conditions.

6.4. A benchmark case: optimal design of a torque arm

There is a classical torque arm problem that was solved by Bennett and Botkin [6] using a local search shape optimization algorithm, which has been resolved by other researchers [38,62,71,84]. This problem, depicted in Fig. 16, may be considered as a benchmark case for a newly proposed shape optimization algorithm. The boundaries of the circular holes and semi-circular arcs, AB and CD, are

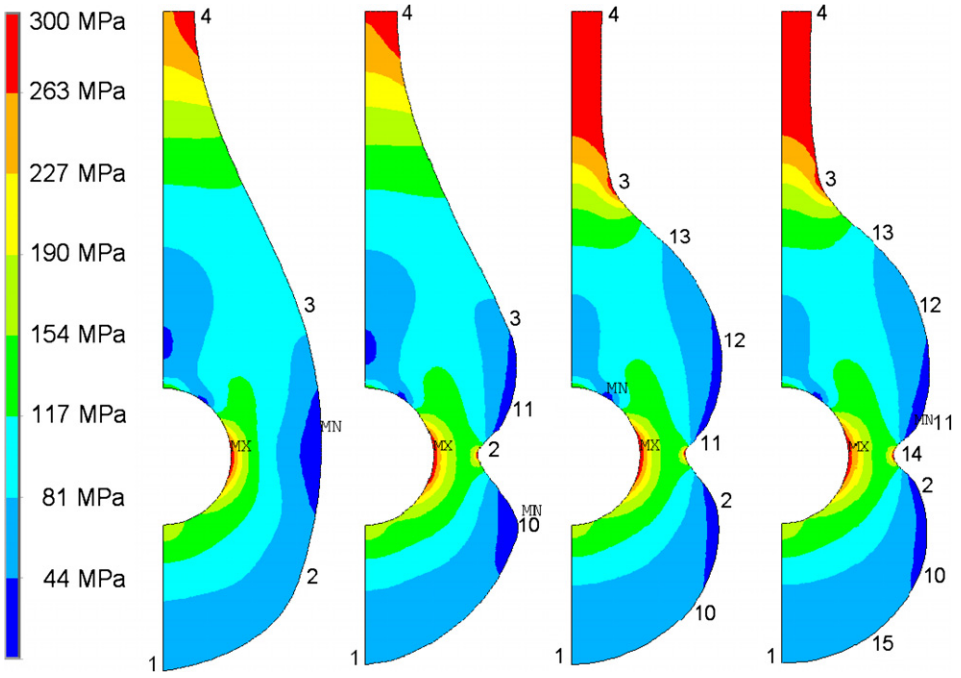


Fig. 14. The optimal shapes found using 4, 6, 8, and 10 key points.

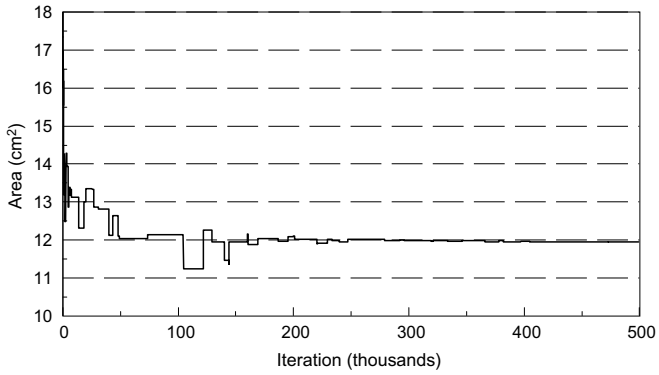


Fig. 15. The change in the lateral area of the best configuration through the optimization process.

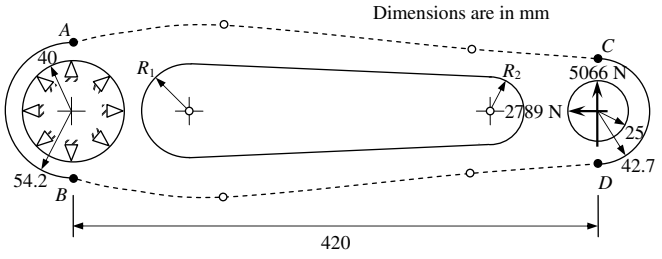


Fig. 16. The classical optimum shape design problem for a torque arm.

not movable. The points A and C, which are not movable, are connected by a spline curve with two moving key points. The inner hole is defined by two semi-circular arcs and two straight lines. The radii of the curvatures and the abscissas of their centers are design variables. Together with the coordinates of the key points on the spline curve, the total number of the design variables is eight. The structure is symmetric with respect to the axis passing through the centers of the holes. Its thickness is 3 mm. The allowable stress of the material is 800 MPa. The boundary of the circular hole on the left is restrained from displacing, while the other is loaded as shown. The 2D model is generated by subtracting the areas of the circular holes and middle hole from the area enclosed by the outer boundary. After the area subtraction, if the number of distinct areas is greater than one, connectivity is assumed to be lost.

Fig. 17 shows the optimal shape of the torque arm generated by the shape optimization algorithm. The lateral area is 156.21 cm^2 and its mass is 0.366 kg. In comparison to the mass of the optimum shape obtained in ref. [62], which was 0.421 kg, this is a significant improvement. Because the inner boundary is defined by arcs connected by lines, which does not provide smooth transition, there is stress concentration at the connection points. This required a very fine mesh as shown in Fig. 18 to correctly calculate the stresses. Shape optimization eliminated stress concentration at the right connection point to a large extent, but at the left it is not totally eliminated, where maximum stress develops. The outer boundary is also not smooth. Nevertheless this did not cause any problem, because the connection points between the arcs and spline curves are within the low stressed regions.

The classical torque arm shape optimization problem poses difficulties of stress concentration in the transition regions between the arcs and spline curves and also leads to optimum designs that may not reflect the features of the best possible design because of the unmovable borders. In order to see the improvement that can be achieved by allowing its entire border to vary, the inner and outer boundaries were define by spline curves with movable key points as shown in Fig. 19. Because of symmetry, the key points on the symmetry axis (A, B, C, and D) may only move along the symmetry axis and the key points on the lower and upper symmetric parts move symmetrically. Thus, there are 16 design variables. The boundary conditions, the material, the thickness of the structure, and the diameter of the holes are the same.

Fig. 20 shows the optimal shape of the torque arm. The lateral area is 124.93 cm^2 and its mass is 0.293 kg. Reduction in weight is significant. Sharp corners occur only at the intersection points between outer (or inner) boundary spline curves and the holes. However, these are not within the highly stressed regions. Significant portion of the left circular support is eliminated. Only a small portion is sufficient to resist the applied loads. This example shows the advantage of using spline curves and allowing the entire

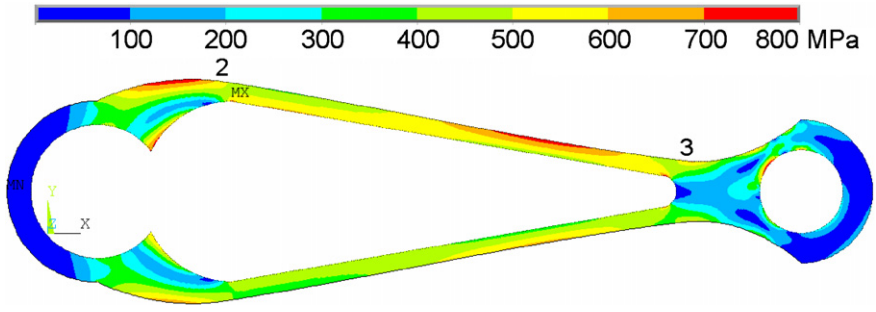


Fig. 17. The optimal shape of the torque arm.

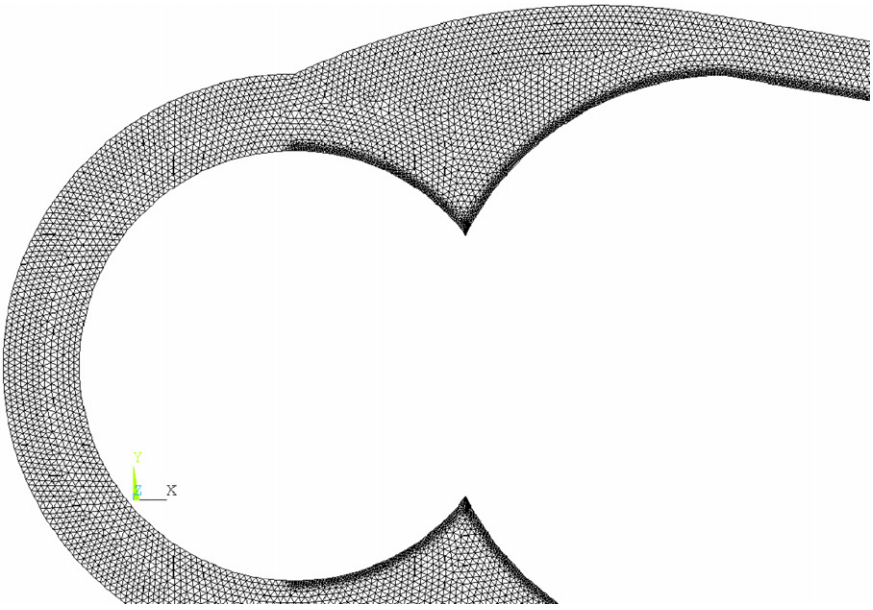


Fig. 18. The finite element mesh used to analyze the torque arm.

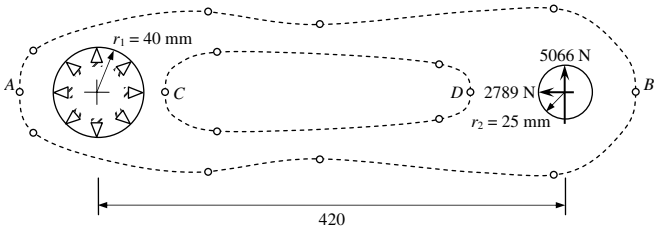


Fig. 19. Optimum shape design of a torque arm with an inner hole.

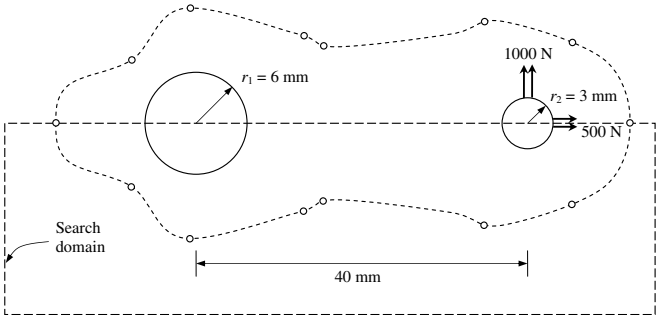


Fig. 21. Optimum design problem for a torque arm.

boundary to vary except the portion of the boundary where the boundary conditions are defined.

6.5. Optimal design of a torque arm

Another problem considered in this study is the optimal design of a torque arm as depicted in Fig. 21, which is similar to the one considered by Shim and Manoochehri [20]. The radii of the circular holes on the left and the right are 6 mm and 3 mm, respectively. The border of the circular hole on the left is restrained from displacing, while the other is loaded as shown. Because concentrated forces are unrealistic and also the high stresses developed at their points of application dominate stress minimization process, these forces are distributed over a number of neighboring nodes. The entire boundary is allowed to move during optimization except that the holes are fixed. Because the structure is symmetric with respect to the axis passing through the centers of the holes, only the coordinates of the key points on one of its sides are design variables, and the two key points on it are constrained to move along this axis. As shown in the figure, the search domain, S, within which the key points can only move, is defined by a rectangle of dimension 75 mm × 22 mm. The allowable stress of the material is taken as 600 MPa.

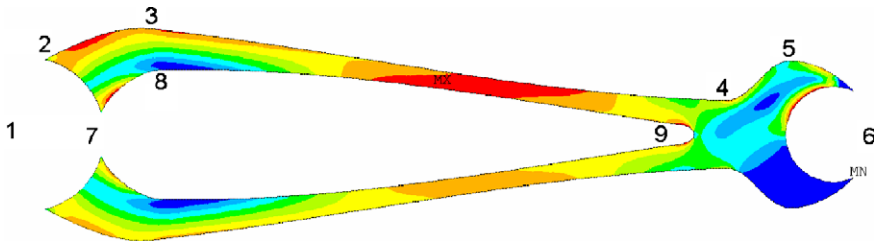


Fig. 20. The optimal shape of the torque arm.

Fig. 22 shows the optimal shapes obtained using 4, 5, 6, 7, 8 and 10 key points. The lateral areas of them were 7.8717, 7.4180, 7.3614, 7.1897, 7.1766, and, 7.1753 cm^2, respectively. The maximum moving distance, R_{max}, was initially 6 mm, and towards the end of the optimization process, it decreased to a value of 0.040 mm. As expected, more precisely defined boundaries result in better shapes with smaller areas. Also, consecutively generated shapes are observed to be similar, implying convergence towards the best configuration. A hump appears close to the larger hole when the number of key points is greater than 6.

Although, the same geometry, material, and boundary conditions were used as in the study conducted by Shim and Manoochehri [20], the results are not comparable. They performed a topology not shape optimization; also they did not allow the material around the holes to be removed.

6.6. How practicable is global search using a local search algorithm?

We know that computational burden of global search algorithms is considerable, while local search algorithms may converge in a few hundred iterations. Then, we need to investigate whether local search algorithms are better alternatives to global search, which may be achieved by repeated runs each time starting from a different initial configuration.

Although first or second order algorithms are more efficient, they are not suitable for global search in shape optimization. Because, it is very likely that connectivity of the structure is lost during iterations. In that case, cost can not be calculated; only a large penalty value can be assigned as cost. Then, derivative of the objective function can not be calculated. For this reason, first and second order local search algorithms may only be employed to improve a current design. Therefore, we are left with zero order methods, which only require calculation of objective function values corresponding to a given set of optimization variables. Among them, Nelder–Mead method was chosen and employed repeatedly starting from arbitrarily generated initial shapes. Fig. 23 shows the lateral areas of the generated optimum shapes. Every one of them had a larger area than the one obtained by the global search algorithm. The optimization process was repeated 350 times, which required more than 200 thousand FE analyses of the structure. Therefore, global search through a local search algorithm is also not computationally efficient; the number of times the algorithm requires calculation of the value of the objective function is about in the same range as the number the global search requires. The reason for this is obvious if one examines the shape in Fig. 24, which suggests that there are infinitely different ways a local optimum shape can show itself. Fig. 25 shows the best shape found by Nelder–Mead algorithm. This has a lateral area of 7.5040 cm^2, which is about 4% larger than the best area

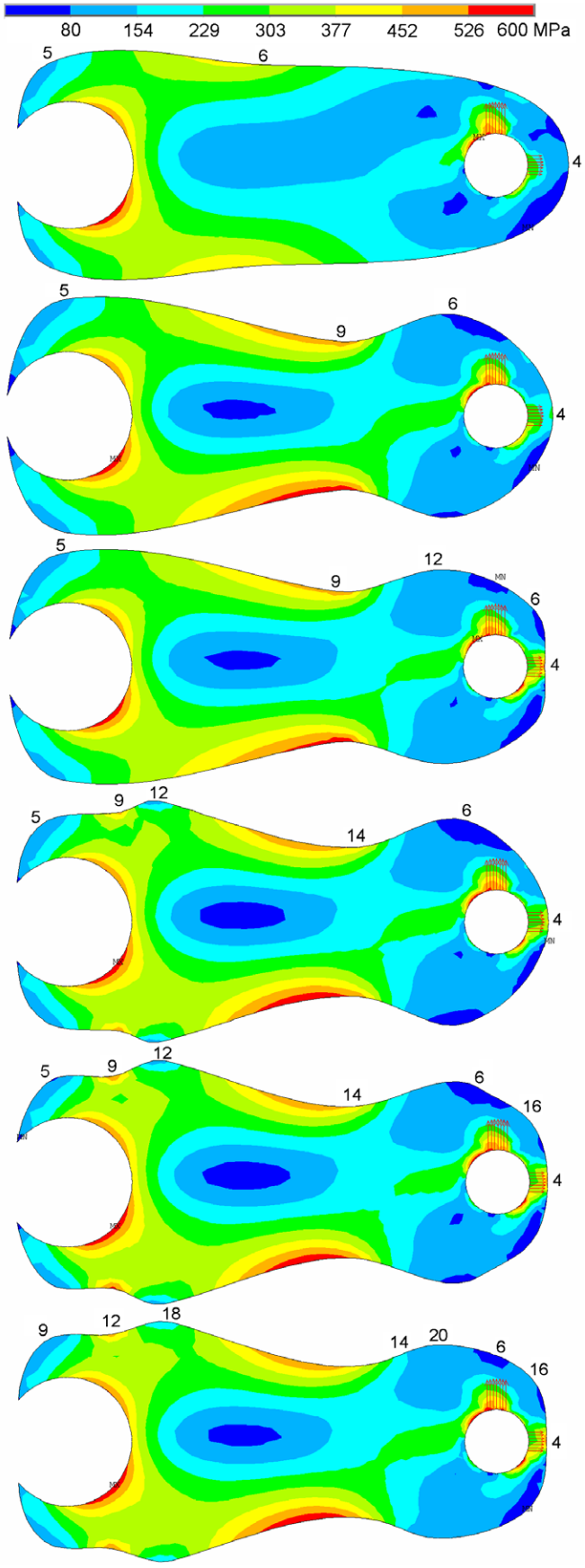


Fig. 22. The optimal shapes found using 4, 5, 6, 7, 8 and 10 key points.

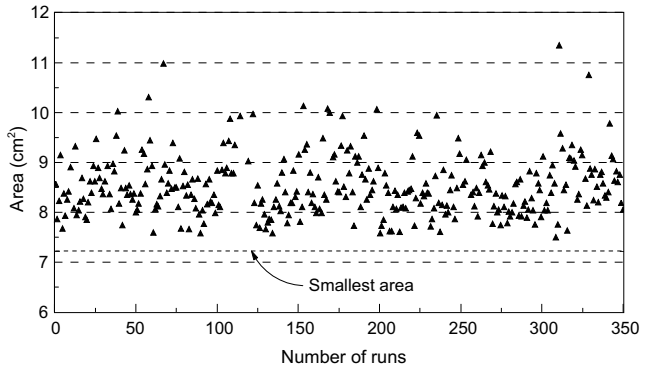


Fig. 23. Lateral areas of the optimum shapes generated through repeated runs using Nelder–Mead algorithm each starting with randomly generated initial shapes.

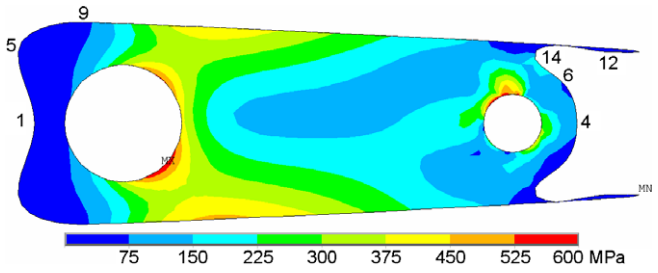


Fig. 24. A typical shape found by a local search algorithm (Nelder–Mead), which is trapped into a local minimum with a high cost.

found by the global search algorithm, DSA. This implies that starting with arbitrary shapes, it is very unlikely for a local search algorithm to locate the globally optimum shape. Also, precision and accuracy can not be checked. Accordingly, we may conclude that a local search algorithm is not suitable for global search in shape optimization problems.

6.7. Towards a more efficient algorithm

As Fig. 15 indicates, large numbers of objective function evaluations are required for global search with DSA. Because FE analysis of a linearly elastic 2D structure takes only a few seconds, this poses no problem during the shape optimization process of 2D structures; but for nonlinear or 3D structures, computational time becomes too long for the implementation of DSA to be practicable in shape optimization. Consequently, we need a more efficient optimization procedure.

There are a number of ways to increase the efficiency of the shape optimization procedure proposed in this study. First of all, the global search algorithm can be used together with a local search algorithm. One may start with DSA and continue the iterations until the global optimum is approximated. Then, one may continue with a local search algorithm to attain final convergence. Accordingly, the optimization process using DSA was intermittently stopped; a number of configurations were randomly chosen among the current configurations; using them as initial configurations, the shape was optimized using Nelder–Mead algorithm. Fig. 26 shows the change in the lateral area of the best shape during the optimization process conducted using DSA for the problem of optimum torque arm design defined by seven key points. Here, the markers show the areas of the optimum shapes obtained by Nelder–Mead. We observe that global search together with local search is very efficient in obtaining near globally optimum designs at the early stages of the optimization. However, towards the end of the optimization process the improvement achieved by the local search is not significant, since a local optimum is already approximated.

Another way to increase the efficiency is to start the optimization process using the optimum configurations obtained with a smaller number of key points as initial configurations instead of randomly generated ones. This method resulted in improved designs after comparatively small number of iterations; but they were not as good as the ones obtained using randomly generated initial shapes.

Improvements in computational time can be achieved by choosing the search domain more judiciously. After the first optimization run with four key points, the search domain, S, defined by a rectangle of dimension 75 mm $\times$

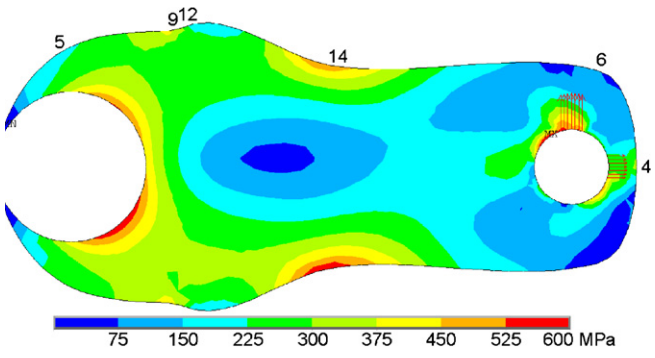


Fig. 25. The best shape found by a local search algorithm (Nelder–Mead).

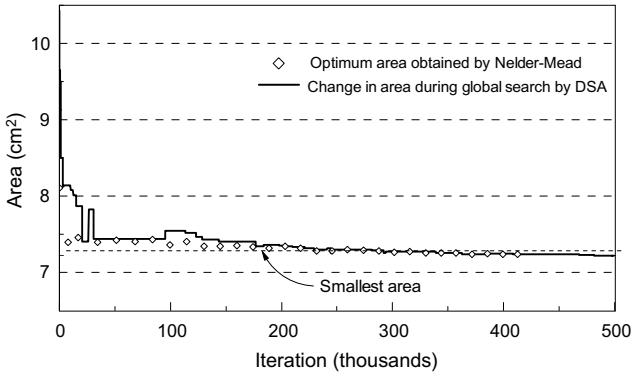


Fig. 26. Solid line shows the change in the lateral area of the best configuration during the optimization process conducted using the global search algorithm, DSA. The markers show the optimum areas obtained by the local search algorithm, Nelder–Mead, using some of the current configurations generated by DSA as initial configurations.

22 mm was found to be too conservative. The algorithm was searching far larger region than necessary. In spite of this, the same search domain was used for optimizing the shapes defined by larger numbers of key points in order to check the reliability of the algorithm. A better procedure would be to modify the search domain taking into account the size of the optimum shape obtained using a small number of key points. Accordingly, a smaller region with a dimension of 57 mm × 10 mm was used for the optimum torque design problem defined by 7 key points. In this case, the optimization process converged to the globally optimum design approximately in about half of the time spent for the case of the larger search domain. Besides, even though approximately the same shape was obtained, this time the optimum shape had a slightly smaller lateral area.

Observing the significance of the size of the search domain, we may further streamline the procedure by assigning different search domains for each key point. After obtaining the optimum shape design defined by a few key points using a single and large search domain, one may define smaller and individual search domains for each key point in optimizing shapes defined by large number of key points. In this way, one may increase the precision of the optimum shape without detracting from the reliability. In order to try this approach, 14 search domains were defined with 2 × 2 mm size for the optimum hook design problem around the chosen 14 nodes on the boundary of the optimum shape defined by 12 key points. However, the initial configurations were not based on this optimum shape; the key points defining these initial configurations were again generated randomly within the search domains. During optimization, if a key point of the best configuration got near the boundary of its search domain, it was extended to allow the free movement of the key point in all directions. As mentioned before, the lateral area of the optimum shape defined by 12 key points was 33.077 cm^2; but the algorithm failed to obtain a better shape when it is defined by 13 key points. Even with a reliable global search algorithm, one may fail to escape local minimums if the search domain is unnecessarily large. This time, even with a 14 key points, the algorithm managed to find a better shape. Fig. 27 shows the optimum shape obtained using 14 key points, its mesh structure and the stress state. The lateral area was obtained to be 32.935 cm^2.

7. Conclusions

In this paper, a 2D shape optimization procedure based on a global search algorithm, DSA, was presented. The only interactive effort expected from a designer is to define the boundary conditions and decide on material, moving boundaries and number of key points. As opposed to most of the methods proposed earlier, which can only improve a current design, the algorithm proposed here can find the globally optimum shape starting from completely arbitrary configurations.

In this study, the importance of precise definition of the optimized system was shown. With a more precise definition of shape, one may find a better optimum design. Another concern is the accuracy of the optimum design, i.e. how well it represents the best possible design. A procedure was proposed to ensure high precision and accuracy, in which starting from a few key points, optimum shapes are found, each time increasing the number of key points, and convergence to the global optimum shape is observed.

Accurate calculation of the cost function was also found to be a crucial factor in the optimum design process. If the FE mesh is not sufficiently refined, consequently the cost

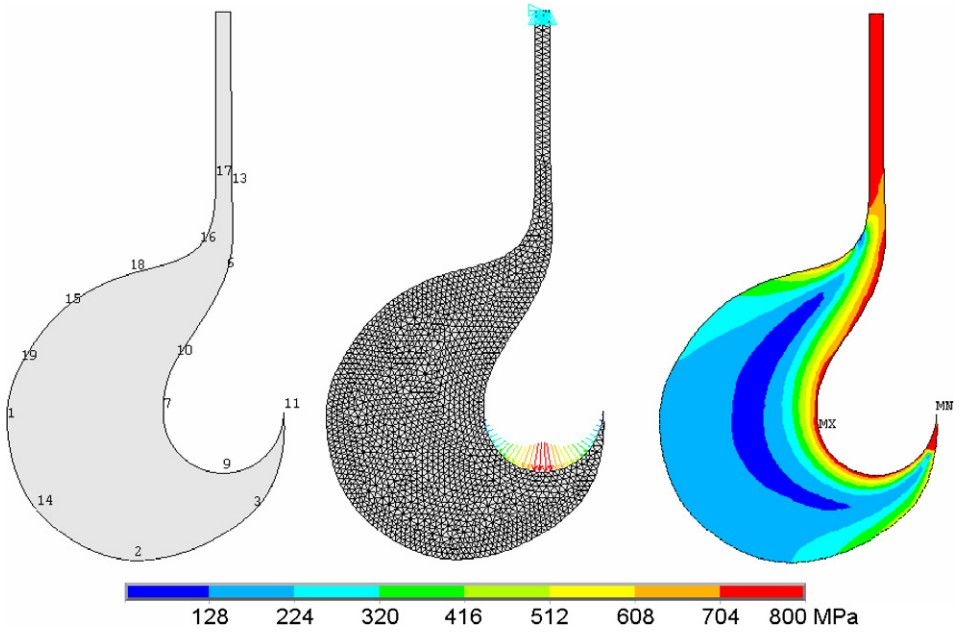


Fig. 27. The optimal shape of the hook defined by 14 key points.

function is not accurately calculated, the resulting shape can not be considered to be optimum.

Careful selection of the search domain was found to be crucial for computational efficiency. If an unnecessarily large search domain is chosen, the algorithm may need quite a number of trials to locate the global minimum. The suggested procedure is that a large search domain is chosen if the shape is defined by a few key points; but when the number of key points is successively increased, a more restricted search domain is used taking into account the size of the optimum shapes defined by a lower number of key points. Finally, a separate and small search domain for each key point is used if the shape is defined by a large number of key points. These search domains are defined around the chosen nodes on the boundary of the optimum designs defined by a lower number of key points. In this way, precision and accuracy can be ensured.

Acknowledgements

This paper is based on the work supported by the Scientific Research Projects of Bogazici University with the code number 01A601.

References

[1] R.T. Haftka, R.V. Grandhi, Structural shape optimization – a survey, Comput. Methods Appl. Mech. Engrg. 57 (1986) 91–106.
[2] J. Mackerle, Topology and shape optimization of structures using FEM and BEM; a biography (1999–2001), Finite Elem. Anal. Des. 39 (2003) 243–253.
[3] E. Schnack, An optimization procedure for stress concentrations by the finite element technique, Int. J. Numer. Methods Engrg. 14 (1979) 115–124.
[4] J.P. Queau, P.H. Trompette, Two-dimensional shape optimal design by the finite element method, Int. J. Numer. Methods Engrg. 15 (1980) 1603–1612.
[5] M.L. Luchi, A. Pogglialini, F. Persiani, An interactive optimization procedure applied to the design of gas turbine discs, Comput. Struct. 11 (1980) 629–637.
[6] J.A. Bennett, M.E. Botkin, Structural shape optimization with geometric description and adaptive mesh refinement, AIAA J. 238 (3) (1984) 458–464.
[7] C.A.M. Soares, H.C. Rodrigues, K.K. Choi, Shape optimal structural design using boundary elements and minimum compliance techniques, Trans. ASME: J. Mech. Trans. Automat. Des. 106 (1984) 518–523.
[8] R.T. Haftka, R.V. Grandhi, Structural shape optimization, Comput. Methods Appl. Mech. Engrg. 57 (1986) 91–106.
[9] Y.K. Shyy, C. Fleury, K. Izadpanah, Shape optimal design using high-order elements, Comput. Methods Appl. Mech. Engrg. 71 (1988) 99–116.
[10] A.D. Belegundu, S.D. Rajan, A shape optimization approach based on natural design variables and shape functions, Comput. Methods Appl. Mech. Engrg. 66 (1988) 87–106.
[11] T.-M. Yao, K.K. Choi, 3-D shape optimal design and automatic finite element regridding, Int. J. Numer. Methods Engrg. 28 (1989) 369–384.
[12] R.J. Yang, Component Shape Optimization Using BEM, Comput. Struct. 37 (4) (1990) 561–568.
[13] P. Hajela, Genetic search – an approach to the nonconvex optimization problem, AIAA J 28 (7) (1990) 1205–1210.
[14] R.J. Yang, M.E. Botkin, Three-dimensional shape optimization with substructuring, AIAA J. 29 (2) (1991) 486–488.
[15] E. Sandgren, E. Jensen, Automotive structural design employing a genetic optimization algorithm, AIAA J. 30 (1992) 920772–920776.
[16] S. Kodiyalam, V. Kumar, P.M. Finnigan, Constructive solid geometry approach to three-dimensional structural shape optimization, AIAA J. 30 (5) (1992) 1408–1415.
[17] G. Anagnostou, E.M. Ronquit, A.T. Patera, A computational procedure for part design, Comput. Methods Appl. Mech. Engrg. 97 (1992) 33–48.
[18] V.E. Theodoracato, J.L. Grimsley, The optimal packing of arbitrarily-shaped polygons using simulated annealing and polynomial-time cooling schedule, Comput. Methods Appl. Mech. Engrg. 125 (1995) 53–70.
[19] A.E. Tekkaya, A. Guneri, Shape optimization with the biological growth method: a parametric study, Engrg. Comput. 13 (8) (1996) 4–18.
[20] P.Y. Shim, S. Manoochehri, Generating optimal configurations in structural design using simulated annealing, Int. J. Numer. Meth. Engrg. 40 (1997) 1053–1069.
[21] E. Kita, H. Tanie, Shape optimization of continuum structures by genetic algorithm and boundary element method, Engrg. Anal. Bound. Elem. 19 (1997) 129–136.
[22] A.V. Cherkaev, Y. Grabovsky, A.B. Movchan, S.K. Serkov, The cavity of the optimal shape under the shear stresses, Int. J. Solids Struct. 35 (33) (1998) 4391–4410.
[23] E. Lund, Shape optimization using Weibull statistics of brittle failure, Struct. Optim. 15 (1998) 208–214.
[24] K. Dems, W. Gutkowski, 2D shape optimization with static and dynamic constraints, Struct. Optim. 15 (1998) 201–207.
[25] A.-V. Phan, S. Mukherjee, J.R.R. Mayer, Stresses, stress sensitivities and shape optimization in two-dimensional linear elasticity by the boundary contour method, Int. J. Numer. Methods Engrg. 42 (1998) 1391–1407.
[26] D. Tran, V. Nguyen, Optimal hole profile in a finite element plate under uniaxial stress by finite element simulation of Durelli's photoelastic stress minimization method, Finite Elem. Anal. Des. 32 (1999) 1–20.
[27] X. Wang, J. Zhou, Y. Hu, A physics-based parameterization method for shape optimization, Comput. Methods Appl. Mech. Engrg. 175 (1999) 41–51.
[28] X. Song, J.D. Baldwin, A novel node-based structural shape optimization algorithm, Comput. Struct. 70 (1999) 569–581.
[29] K. Tai, R.T. Fenner, Optimum shape and topology design using the boundary element method, Int. J. Solids Struct. 36 (1999) 2021–2040.
[30] A.-V. Phan, T.-N. Phan, A structural shape optimization system using the two-dimensional boundary contour method, Arch. Appl. Mech. 69 (1999) 481–489.
[31] W. Annicchiarico, M. Cerrolaza, Finite elements, genetic algorithms and β-splines: a combined technique for shape optimization, Finite Elem. Anal. Des. 33 (1999) 125–141.
[32] M. Heller, R. Kaye, L.R.F. Rose, A gradientless finite element procedure for shape optimization, J. Strain Anal. 34 (5) (1999) 323–336.
[33] R. Kaye, M. Heller, Investigation of shape optimization for the design of life extension options for an F/A-18 Airframe FS 470 bulkhead, J. Strain Anal. 35 (6) (2000) 493–505.
[34] P. Pedersen, On optimal shapes in materials and structures, Struct. Multidisc. Optim. 19 (2000) 169–182.
[35] A. Schleupen, K. Maute, E. Ramm, Adaptive FE-procedures in shape optimization, Struct. Multidisc. Optim. 19 (2000) 282–302.
[36] H. Altinkopru, F.O. Sonmez, Shape optimization of 3D-shell structures using simulated annealing, in: N. Mastorakis (Ed.), Problems in Modern Applied Mathematics, World Scientific and Engineering Society Press, 2000, pp. 135–140.
[37] P. Chaperon, R. Jones, M. Heller, S. Pitt, F. Rose, A methodology for structural optimization with damage tolerance constraints, Engrg. Failure Anal. 7 (2000) 281–300.
[38] S.Y. Han, Shape optimization for general two-dimensional structures, Acta Mech. 145 (2000) 117–125.

[39] J. Herskovits, G. Dias, G. Santos, C.M.M. Soares, Shape structural optimization with an interior point nonlinear programming algorithm, Struct. Multidisc. Optim. 20 (2000) 107–115.
[40] J. Herskovits, A. Leontiev, G. Dias, G. Santos, C.M.M. Soares, Contact shape optimization: a bilevel programming approach, Struct. Multidisc. Optim. 20 (2000) 214–221.
[41] M. Cerrolaza, W. Annicchiarico, M. Martinez, Optimization of 2D boundary element models Using β-splines and genetic algorithms, Engrg. Anal. Bound. Elem. 24 (2000) 427–440.
[42] M. Kegl, Shape optimal design of structures: an efficient shape representation concept, Int. J. Numer. Methods Engrg. 49 (2000) 1571–1588.
[43] W. Waldman, M. Heller, G.X. Chen, Optimal free-form shapes for shoulder fillets in flat plates under tension and bending, Int. J. Fatigue 23 (2001) 509–523.
[44] P. Vinot, S. Cogan, J. Piranda, Shape optimization of thin-walled beam-like structures, Thin-walled Struct. 39 (2001) 611–630.
[45] N. Gunduz, N. Akbulut, F.O. Sonmez, Generating optimal 2D structural designs using simulated annealing, in: S. Hernandez, C.A. Brebbia (Eds.), Computer Aided Optimum Design of Structures, vol. VII, WIT Press, 2001, pp. 347–356.
[46] D. Hilding, B. Torstenfelt, A. Klarbring, A computational methodology for shape optimization of structures in frictionless contact, Comput. Methods Appl. Mech. Engrg. 190 (2001) 4043–4060.
[47] W. Annicchiarico, M. Cerrolaza, Structural shape optimization 3D finite-element models based on genetic algorithms and geometric modeling, Finite Elem. Anal. Des. 37 (2001) 403–415.
[48] S.Y. Woon, O.M. Querin, G.P. Steven, Structural application of a shape optimization method based on a genetic algorithm, Struct. Multidisc. Optim. 22 (2001) 57–64.
[49] L. Qing, G.P. Steven, O.M. Querin, Y.M. Xie, Stress based optimization of torsional shafts using and evolutionary procedure, Int. J. Solids Struct. 38 (2001) 5661–5677.
[50] H.S. Hedia, Shape optimisation to maximize crack initiation time, Bio-Medical Mater. Engrg. 11 (2001) 293–300.
[51] F. Bobaru, S. Mukherjee, Shape sensitivity analysis and shape optimization in planar elasticity using the element-free Galerkin method, Comput. Methods Appl. Mech. Engrg. 190 (2001) 4319–4337.
[52] S. Butkewitsch, V. Steffen, Shape optimization, model updating and empirical modeling applied to the design synthesis of a heavy truck side guard, Int. J. Solids Struct. 39 (2002) 4747–4771.
[53] J.A.T. Freitas, I. Cismasiu, Shape optimization with hybrid – Trefftz displacement elements, Int. J. Numer. Methods Engrg. 53 (2002) 473–498.
[54] I. Paczelt, T. Szabo, Solution of contact optimization problems of cylindrical bodies using HP-FEM, Int. J. Numer. Methods Engrg. 53 (2002) 123–146.
[55] S.-Y. Han, J.-K. Lim, Shape optimization for prolonging fatigue life, JSME Int. J.: Ser. A 45 (2) (2002) 298–304.
[56] P. Beremlijski, J. Haslinger, M. Kocvara, J. Outrata, Shape optimization in contact problems with Coulomb friction, Soc. Ind. Appl. Math. 13 (2) (2002) 561–587.
[57] T. Burcynski, A. Dlugosz, Evolutionary optimization in thermoelastic problems using the boundary element method, Comput. Mech. 28 (2002) 317–324.
[58] F. Bobaru, S. Mukherjee, Meshless approach to shape optimization of linear thermoelastic solids, Struct. Multidisc. Optim. 53 (2002) 765–796.
[59] E. Schnack, W. Weikl, Shape optimization under fatigue using continuum damage mechanics, Comput.-Aided Des. 34 (2002) 929–938.
[60] A. Tafreshi, Shape design sensitivity analysis of 2D anisotropic structures using the boundary element method, Engrg. Anal. Bound. Elem. 26 (2002) 237–251.
[61] J. Lampinen, Cam shape optimization by genetic algorithm, Comput.-Aided Des. 35 (2003) 727–737.
[62] N.H. Kim, K.K. Choi, M.E. Botkin, Numerical method for shape optimization using meshfree method, Struct. Multidisc. Optim. 24 (2003) 418–429.
[63] J. Shen, D. Yoon, A new scheme for efficient and direct shape optimization of complex structures represented by polygonal meshes, Int. J. Numer. Methods Engrg. 58 (2003) 2201–2223.
[64] S.Y. Woon, L. Tong, O.M. Querin, G.P. Steven, Knowledge-based algorithms in fixed-grid GA shape optimization, Int. J. Numer. Methods Engrg. 58 (2003) 643–660.
[65] M. Özakça, N. Tayşi, F. Kolcu, Buckling analysis and shape optimization of elastic variable thickness circular and annular plates – II. Shape optimization, Engrg. Struct. 25 (2003) 193–199.
[66] C. Wessel, A. Cisilino, B. Sensale, Structural shape optimisation using boundary elements and the biological growth method, Struct. Multidisc. Optim. 28 (2004) 221–227.
[67] S.A. Falco, S.M.B. Afonso, L.E. Vaz, Analysis and optimal design of plates and shells under dynamic loads – II: optimization, Struct. Multidisc. Optim. 27 (2004) 197–209.
[68] M. McDonald, M. Heller, Robust shape optimization of notches for fatigue-life extension, Struct. Multidisc. Optim. 28 (2004) 55–68.
[69] S. Hyun, C. Kim, J.H. Son, S.H. Shin, Y.S. Kim, An efficient shape optimization method based on fem and B-spline curves and shaping a torque converter clutch disk, Finite Elem. Anal. Des. 40 (2004) 1803–1815.
[70] M.J. Garcia, C.A. Gonzales, Shape optimisation of continuum structures via evolution strategies and fixed grid finite element analysis, Struct. Multidisc. Optim. 26 (2004) 92–98.
[71] G.-W. Jang, Y.Y. Kim, K.K. Choi, Remesh-free shape optimization using the wavelet-Galerkin method, Int. J. Solids Struct. 41 (2004) 6465–6483.
[72] A.A. Mailybaev, H. Yabuno, H. Kaneko, Optimal shapes of parametrically excited beams, Struct. Multidisc. Optim. 27 (2004) 435–445.
[73] J. Norato, R. Haber, D. Tortorelli, M.P. Bendsoe, A geometry projection method for shape optimization, Int. J. Numer. Methods Engrg. 60 (2004) 2289–2312.
[74] M. Haiba, D.C. Barton, P.C. Brooks, M.C. Levesley, Evolutionary structural optimization of dynamically loaded components in consideration of fatigue life, Adv. Engrg. Software 36 (2005) 49–57.
[75] W.L. Li, Q. Li, G.P. Steven, Y.M. Xie, An evolutionary shape optimization for elastic contact problems subject to multiple load cases, Comput. Methods Appl. Mech. Engrg. 194 (2005) 3394–3415.
[76] E. Cervera, J. Trevelyan, Evolutionary structural optimization based on boundary representation of NURBS. Part 1: 2D algorithms, Comput. Struct. 83 (2005) 1902–1916.
[77] F. Schmid, K. Hirschen, S. Meynen, M. Schafer, An enhanced approach for shape optimization using an adaptive algorithm, Finite Elem. Anal. Des. 41 (2005) 521–543.
[78] J.-S. Liu, G.T. Parks, P.J. Clarkson, Topology/shape optimization of axisymmetric continuum structures – a metamorphic development approach, Struct. Multidisc. Optim. 29 (2005) 73–83.
[79] Z.Q. Zhang, J.X. Zhou, N. Zhou, X.M. Wang, L. Zhang, Shape optimization using kernel particle method and an enriched genetic algorithm, Comput. Methods Appl. Mech. Engrg. 194 (2005) 4048–4070.
[80] R. Das, R. Jones, Y.M. Xie, Design of structures for optimal static strength Using ESO, Engrg. Failure Anal. 12 (2005) 61–80.
[81] I.Y. Shevtsov, V.L. Markine, C. Esveld, Optimal design of wheel profile for railway vehicles, Wear 258 (2005) 1022–1030.
[82] M.-H. Chang, C.-H. Cheng, Optimal design of slider shape for satisfying load demands under specified operation conditions, Tribol. Int. 38 (2005) 757–768.
[83] R. Meske, J. Sauter, E. Schnack, Nonparametric gradient-less shape optimization for real-world applications, Struct. Multidisc. Optim. 30 (2005) 201–218.
[84] N.H. Kim, Y. Chang, Eulerian shape design sensitivity analysis and optimization with a fixed grid, Comput. Methods Appl. Mech. Engrg. 194 (2005) 3291–3314.

[85] R. Jones, D. Peng, P. Chaperon, S. Pitt, D. Abramson, T. Peachey, Structural optimisation with damage tolerance constraints, Theor. Appl. Fract. Mech. 43 (2005) 133–155.
[86] F.O. Sonmez, Precision and accuracy in generating globally optimum shapes, in: I. Garcia, L.G. Casado, E.M.T. Hendrix, B. Toth (Eds.), Proceedings of the International Workshop on Global Optimization, San Jose, Spain, pp. 231–236, 2005.
[87] Z. Wu, An efficient approach for shape optimization of components, Int. J. Mech. Sci. 47 (2005) 1595–1610.
[88] H.H. Yoo, J.E. Cho, J. Chung, Modal analysis and shape optimization of rotating cantilever beams, J. Sound Vibr. 290 (2006) 223–241.
[89] S. Kirkpatrick, C.D. Gelatt, M.P. Vecchi, Optimization by simulated annealing, Science 220 (1983) 671–680.
[90] M.M. Ali, A. Törn, S. Viitanen, A direct search variant of the simulated annealing algorithm for optimization involving continuous variables, Comput. Operat. Res. 29 (2002) 87–102.